International Journal of Innovative Technology and Exploring Engineering (IJITEE)
ISSN: 2278-3075, Volume-8 Issue-8, June 2019

Application of Response Surface Methodology in Investigating Cladding of Steel using Gas Metal Arc Welding

Miniappan. P.K

Abstract: Cladding is a surfacing method by a Gas Metal Arc Welding (GMAW), on carbon or low composite steel base metal to perk up its wear obstruction property. GMAW is utilized for cladding. The properties of clad portions rely on the weld geometry and welding parameters, which must be controlled. Microsoft Excel Solver has been used to streamline the parameters to achieve least debilitating, most extraordinary help, least passageway, most prominent weld width to a target motivating force with the point of view of overseeing on material and to achieve the appealing clad estimations. The work was finished using 309LSi tempered steel filler wire of 0.9mm with IS:2062 assistant steel plates of 20mm thickness as base plates, under the guard of 95% Argon and 5% of Hydrogen gas blend.

Index Terms: Cladding; Gas metal arc welding; Microsoft Excel Solver; stainless steel

I. INTRODUCTION

Modern parts are experiencing wear and erosion [1]. To broaden the life of the segment ordinarily, cladding is connected, which is conservative moreover [2]. Low carbon or medium carbon composite steel with clad material will meet the prerequisite in specialized and money related grounds [2-4].Cladding is a prominent surfacing procedure wherein a thick material layer takes care of a generally low expense basic material to upgrade its mechanical properties just as consumption opposition properties to build service life [5]. Cladding is where one material covers another either inside or remotely [6]. This kind of procedure is utilized with metallic materials, optical filaments, development materials, and so forth. Metal cladding is a kind of outside covering made of metallic material and its thickness is around 10 to 20% of all-out clad plate thickness. They are composites of at least two metals participated in a nonstop way by a metallic bond. Liner is another sort of spread wherein the joining type is discontinuous. Clad metals are broadly utilized in the chemical, oil, atomic, maritime, aeronautical, service and support enterprises [7-9]. RSM is a strategy to decide and speak to the circumstances [10-13] and logical results connection between obvious mean reactions and info control factors affecting the reactions as a few dimensional hypersurfaces [14-19]. The precision and viability of a test program rely upon cautious arranging and execution of the exploratory systems [20-23]. This research work carried out on a bead on the plates using 0.9mm diameter of309LSI SS consumable electrode wire on the steel plate of IS2062 under the Argon 95% Hydrogen 5% blend. The objectives of this work are as follows;

Revised Manuscript Received on June 7, 2019

Miniappan.P.K, Assistant Professor, Department of Automobile Engineering, Karpagam Academy of Higher Education, Coimbatore-641021, INDIA.

- Identifying the significant procedure control factors and finding their higher and lower limits.
- Recording the reactions viz., entrance (DP), dot width (W), support (R) and computing percentage weakening (D).
- Developing a scientific model, deciding the coefficient of the relapse model.
- Presenting the impacts of procedure parameters in graphical structure and investigating the outcomes.

II. MATERIALS AND METHODS

Table 1 and Table 2 provide the details of the base plate and filler material. The process control factors and its levels are specified in Table 3.

Table 1: Steel plate composition

Material	Elements %			
	C	Mn	S	P
IS:2062	0.25	1.5	0.05	0.05

Table 2: Chemical composition of clad metal

Material	Elements %						
	P	Mn	S	C	Si	Ni	Cr
ER-309LSi	0.023	2.14	0.006	0.025	0.52	13.67	23.14

A. Identification of higher and lower limits of a process control variable

a) Response measurement for the welding parameters (A), welding current (I), welding speed (B), plate to nozzle distance (N)
b) Identification of higher and lower limits
c) Regression model development
d) Analysis of results

Table 3: Procedure Control components and its Levels

Variables	*Notations*	*Variables Level*				
		-1.682	**-1**	**0**	**1**	**1.682**
Current applied (A)	I	130	134.05	140	145.94	150
Welding speed (cm/min)	B	13.94	16.55	20.39	24.23	26.84
plate to nozzle distance (mm)	N	6	8.43	12	15.56	18

Published By:
Blue Eyes Intelligence Engineering
& Sciences Publication

B. Measurement of the data

Based on the design of the experiment, the run was carried out randomly to avoid errors. The plates were cut and samples were taken and shown in Figure 1 and Figure 2. 'W' width of bead, 'DP' penetration and 'R' reinforcement are made available using AUTOCAD. The area of weld geometry to penetration, bead area, and dilution arrived. Twenty experiments in number were conducted using the design of experiments. The plane plates were sliced at their mediocre for test examples of 15 mm width. These examples were cleaned and weld dab profiles were dissected by utilizing an optical profile projector and the dab profiles viz., (W), (DP), (R) were estimated. To ascertain the percent weakening (D) the watched and determined estimations of the globule parameters and weakening are given in Table 4. Figure 1, Figure 2 and Figure 3 demonstrate the run of the mill clad examples, weld dot cross areas, and weld dot geometry separately.

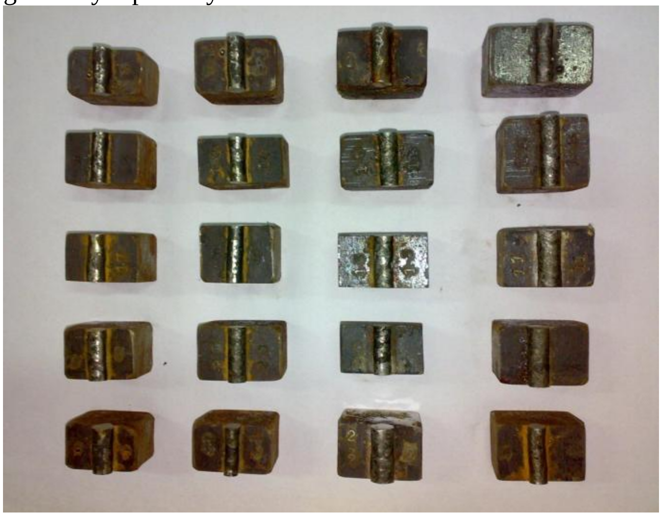

Figure 1: Photograph of cladded specimens

Figure 2: Typical cladding cross sections

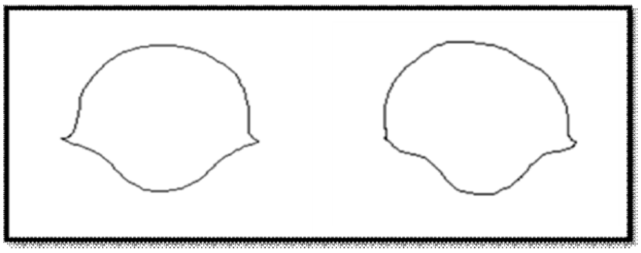

Figure 3: Typical geometry of profiles

III. RESULTS AND DISCUSSIONS

Table 4: Structure Matrix and watched estimations of globule geometry

Expt. run	Structure Matrix			Bead geometry and dilution			
	I (A)	B (cm/min)	N (mm)	DP (mm)	R (mm)	W (mm)	D (%)
1	-1	-1	-1	1.77	4.33	6.99	21.46
2	1	-1	-1	2.2	4.53	7.92	25.35
3	-1	1	-1	1.86	3.33	6.18	30
4	1	1	-1	2.26	3.74	6.19	32.02
5	-1	-1	1	1.67	4.8	6.03	18.56
6	1	-1	1	1.03	3.31	6.53	23
7	-1	1	1	1.35	3.6	5.08	22.78
8	1	1	1	1.98	4.04	5.69	25.85
9	-1.682	0	0	1.6	3.47	5.57	27.5
10	1.682	0	0	2.13	4.72	6.74	23.71
11	0	-1.682	0	2.41	4.68	6.92	23.82
12	0	1.682	0	1.92	4.06	5.31	27.51
13	0	0	-1.682	2.08	3.82	6.77	29.55
14	0	0	1.682	1.66	4.27	5.55	21.6
15	0	0	0	1.81	4.14	6.12	23.74
16	0	0	0	1.96	3.82	6.05	28.96
17	0	0	0	1.89	4.02	6.16	26.47
18	0	0	0	1.82	4.16	5.78	23.49
19	0	0	0	1.8	4.19	6.02	23.61
20	0	0	0	1.9	4.11	6.39	25.03

A. *Regression model development*

The delegate reaction capacity of the weld dab measurements can be communicated as

Y= f (I, B, N) (1)

The second request polynomial condition for the reaction surface for k components is

$$y = b_0 + \sum_{i=1}^{k} b_i x_i + \sum_{i=1}^{k} b_{ii} x_i^2 + \sum_{i,j=1, j\neq i}^{k} b_{ij} x_i x_j \quad (2)$$

Where, z0 is the free term, the coefficients z1,z2,… zk are straight terms, the coefficients z11, z22,…zkk are quadratic terms and coefficients z12, z13,… .zk-1,k are the communication terms. For three factors, the chose polynomial could be communicated as

$$Y = z_0 + z_1 I + z_{2B} + z_3 N + z_{11} I^2 + z_{22B}^{2} + z_{33} N^2 + z_{12} IB + z_{13} IN + z_{23BN} \quad (3)$$

B. *Assessment of coefficients of representation*

The estimations of the coefficients of the above polynomial were arrived utilizing QA six sigma measurable programming (DOE-PC IV), Table 5 demonstrates the assessed coefficients.

Table 5: Calculation coefficients of Regression analysis for bead parameters

Coefficient	Estimations of coefficients			
	DP	R	W	D
z_0	1.870	4.080	6.081	25.241
z_1	0.125	0.122	0.294	0.516
z_2	-0.003	-0.242	-0.515	2.086
z_3	-0.203	0.042	-0.439	-2.344
z_{11}	-0.043	-0.038	0.062	-0.023
z_{22}	0.063	0.059	0.048	-0.002

Published By:
Blue Eyes Intelligence Engineering
& Sciences Publication

z_{33}	-0.041	-0.056	0.064	-0.034
z_{12}	0.155	0.268	-0.101	-0.405
z_{13}	-0.105	-0.208	0.021	0.200
z_{23}	0.060	0.165	0.094	-1.017
DP= Depth of penetration, R=Reinforcement, W=Width of the bead D=Dilution				

C. Development of final models

The significant co-efficient were considered for arriving the suitable regression model and bead geometry is provided below;

The anticipated Regression models for globule geometry are given beneath:

$$DP=1.855+0.125I–0.203N+0.155IS–0.105IN \quad (4)$$

$$R=4.057+0.122I–0.242S+0.268IS+0.208IN+0.165SN \quad (5)$$

$$W=6.199+0.294I–0.515S–0.439N–0.101IS+0.094SN \quad (6)$$

$$D=25.201+2.086S–2.344N–1.017SN \quad (7)$$

D. Model Validity

The different values are assigned to process variables which are different from design matrixes but within the working limits and tests are conducted compared with actual and predicted results of response and tabulated in Table 5 Such results were found to be satisfactory.

E. Consequences of control factors on bead geometry

Figure 4 (a) demonstrates the immediate impact of welding current on globule geometry. Increment in the present lead to increment in the entrance. As current builds, the warmth info increments bringing about higher current thickness causing bigger volume of the base plate softening and consequently entrance; increment in current outcomes in expanded fortification, it was discovered that the wire feed rate is legitimately corresponding to welding current, as welding current builds wire feed rate is expanded subsequently more measure of metal is kept per unit length; globule width increments with an expansion in current. Figure 4 (b) demonstrates the immediate impact of welding speed on dot geometry. Welding pace does not fundamentally influence the entrance; as the welding pace builds less measure of clad metal per unit length is saved on the base metal. This causes abatement in support; dab width diminishes as the welding velocity increments. Figure 4 (c) demonstrates the immediate impact of spout to-plate separate on dot geometry. Increment in a spout to plate separation diminishes entrance. This might be because of the decline in welding current with the expansion in 'N'. As terminal augmentation expands the circuit opposition increments and the welding current drops. This is because of a lessening in the welding current. This decrease in welding current is because of an expansion in circuit obstruction. The drop in current outcomes in diminished base metal liquefying and consequently, weld dab width diminishes; percent weakening abatements with an expansion in 'N'. As talked about above, as terminal augmentation builds the circuit opposition increments and the welding current drops. The yield voltage of the power source stays steady. In this manner, more voltage drop over the expansion and subsequently less voltage happen over the circular segment. The reduction in both voltage and current may decrease the entrance of the circular segment and henceforth lessen weakening.

Welding speed=20.395cm/min
Nozzle to plate distance=12mm

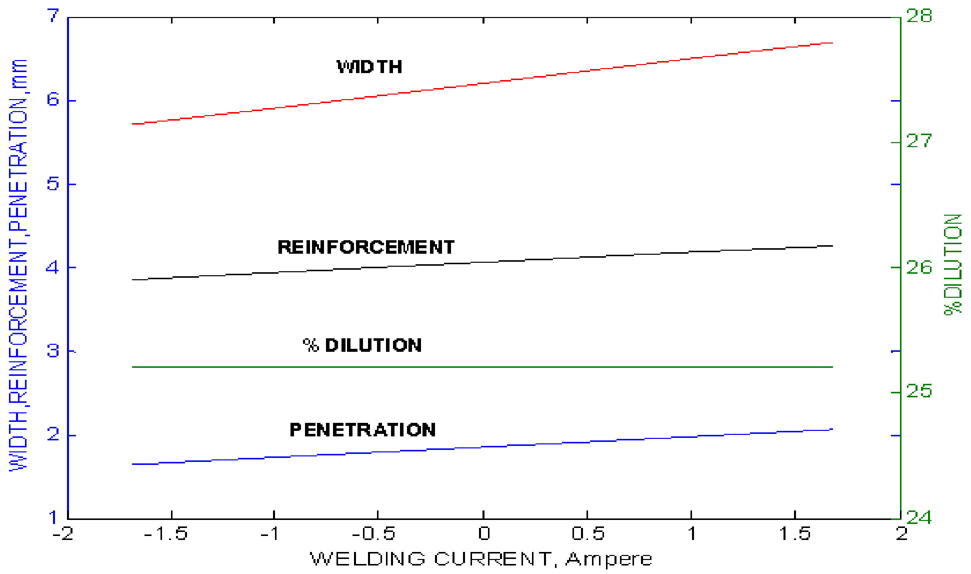

Figure 4(a): Influence of Welding Current on Bead Geometry

Published By:
Blue Eyes Intelligence Engineering
& Sciences Publication

Nozzle to plate distance=12mm

Welding current=140A

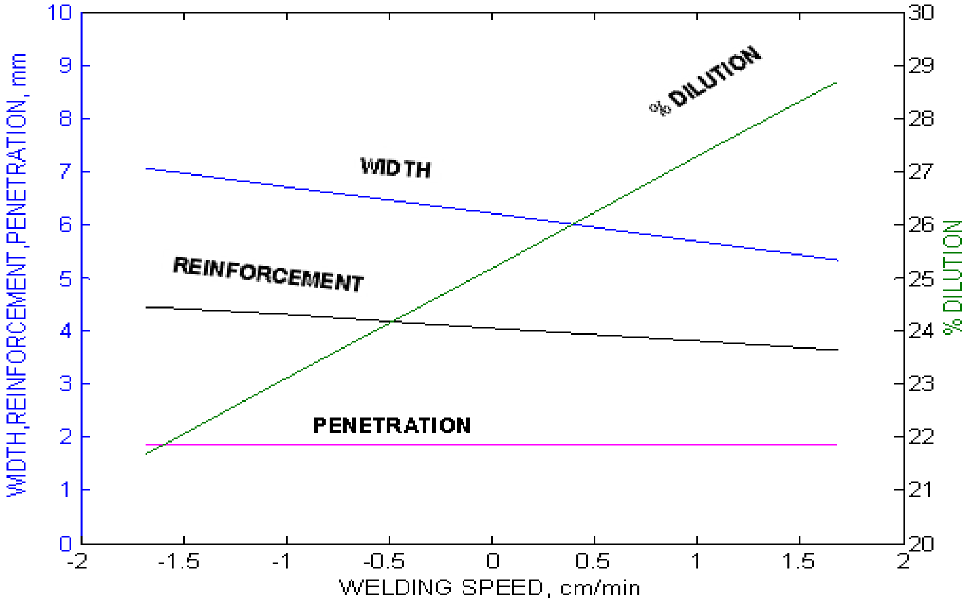

Figure 4(b): Influence of Welding Speed on Bead Geometry

Welding current=140A Welding speed=20.395cm/min

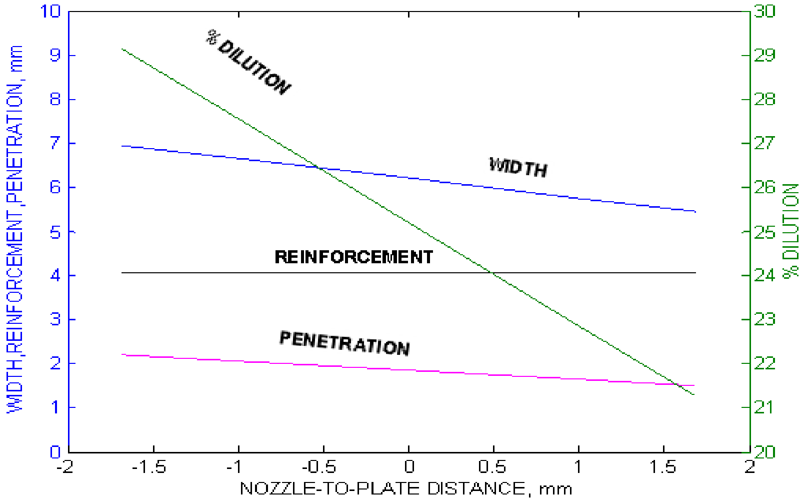

Figure 4(c): Influence of plate-to-nozzle distance on Geometry of Bead

Once the regression model was developed then Gas Metal Arc Welding process could be optimized. Achieving the desired weld quality with the minimum cost was identified as the goal. The improvement was done utilizing Microsoft Excel Solver programming. The bead parameters were enhanced freely by thinking about their conditions as individual target capacities for cladding, dot entrance ought to be least, fortification ought to be greatest, globule width ought to be most extreme and weakening ought to be least. The dot geometry parameters were advanced subject to the accompanying imperatives:

-1.682<I<1.682; -1.682<S<1.682; -1.682<N<1.682

And the optimized solutions obtained after several iterations are tabulated below.

Table 6: Optimum Process Parameters

Best control factors	**Minimize the depth of Penetration**	**Maximize the reinforcement**	**Maximize the bead width**	**Minimizing the percent dilution**
I Current in (A)	1.682 (150A)	1.682 (150A)	1.682 (150A)	1.682 (150A)
S Welding Speed(cm/min)	1.682 (13.94cm/min)	1.682 (13.94cm/min)	1.682 (13.94cm/min)	1.682 (13.94cm/min)
N Plate to Nozzle distance	-1.682 (6mm)	1.682 (18mm)	-1.682 (6mm)	1.682 (18mm)
P Predicted Response	R=4.966mm	P=0.988mm	W=8.849mm	D=20.627%

Published By:
Blue Eyes Intelligence Engineering
& Sciences Publication

IV. CONCLUSIONS

The Analytical examination utilizing Microsoft programming has brought about the accompanying end. The enhanced procedure parameters, for example, welding current, welding speed, spout to plate separation to acquire the ideal weld pool geometry and weld quality. The impact of procedure factors demonstrate

- Increase in welding current causes a slight increment in infiltration and fortification
- If weld speed builds the level of weakening likewise increments yet does not influence the entrance
- Reinforcement and weld globule width diminishes with the expansion in weld speed.
- Depth of entrance, weld globule width and rate weakening abatements, with increment in plate to spout separate

Nomenclature

GMAW	-	Gas Metal Arc Welding
RSM	-	Response Surface Methodology
mm	-	millimeter
DP	-	Penetration
W	-	Bead width
Ni	-	Nickel
R	-	Reinforcement
Si	-	Silicon
D	-	Percentage of dilution
C	-	Carbon
cm/min	-	centimeter per minute
P	-	Phosphorous
A	-	Current applied
Cr	-	Chromium
B	-	Welding speed
S	-	Sulphur
N	-	Plate to nozzle distance
A	-	Ampere
Mn	-	Manganese

REFERENCES

1. Cui, S., Miao, Q., Liang, W., Xu, Y. and Li, B., 2017. Comparative analysis of tribological behavior of plasma-and high-velocity oxygen fuel-sprayed WC-10Co-4Cr coatings. *Industrial Lubrication and Tribology*, *69*(2), pp.325-332.
2. Yin, S., Xie, Y., Cizek, J., Ekoi, E.J., Hussain, T., Dowling, D.P. and Lupoi, R., 2017. Advanced diamond-reinforced metal matrix composites via cold spray: properties and deposition mechanism. *Composites Part B: Engineering*, *113*, pp.44-54.
3. Crouch, I.G., Sandlin, J. and Thomas, S., 2017. Polymers and fibre-reinforced plastics. In *The Science of Armour Materials*(pp. 203-268). Woodhead Publishing.
4. Schmidt, M., Zaeh, M., Li, L., Duflou, J., Overmeyer, L. and Vollertsen, F., 2018. Advances in macro-scale laser processing. *CIRP Annals*, *67*(2), pp.719-742.
5. Brownell, B., 2017. *Transmaterial next: A catalog of materials that redefine our future*. Chronicle Books.
6. Mahamood, R.M., 2018. *Laser metal deposition process of metals, alloys, and composite materials*. Cham: Springer.
7. Jędrzejewska-Szczerska, M., Majchrowicz, D., Hirsch, M., Struk, P., Bogdanowicz, R., Bechelany, M. and Tuchin, V.V., 2018. Nanolayers in Fiber-Optic Biosensing. In *Nanotechnology and Biosensors* (pp. 395-426).
8. Youheng, F., Guilan, W., Haiou, Z. and Liye, L., 2017. Optimization of surface appearance for wire and arc additive manufacturing of Bainite steel. *The International Journal of Advanced Manufacturing Technology*, *91*(1-4), pp.301-313.
9. Honarpisheh, M., Jobedar, M.M. and Alinaghian, I., 2018. Multi-response optimization on single-point incremental forming of hyperbolic shape Al-1050/Cu bimetal using response surface methodology. *The International Journal of Advanced Manufacturing Technology*, *96*(9-12), pp.3069-3080.
10. Selvam, M.D., Srinivasan, V. and Sekar, C.B., 2014. An attempt to minimize lubricants in various metal cutting processes. *International Journal of Applied Engineering Research*, *9*(22), pp.7688-7692.
11. Selvam, M.D., Dawood, D.A.S. and Karuppusami, D.G., 2012. Optimization of machining parameters for face milling operation in a vertical CNC milling machine using genetic algorithm. *IRACST-Engineering Science and Technology: An International Journal (ESTIJ)*, *2*(4).
12. Selvam, M.D. and Senthil, P., 2016. Investigation on the effect of turning operation on surface roughness of hardened C45 carbon steel. *Australian Journal of Mechanical Engineering*, *14*(2), pp.131-137.
13. Selvam, M.D., Senthil, P. and Sivaram, N.M., 2017. Parametric optimisation for surface roughness of AISI 4340 steel during turning under near dry machining condition. *International Journal of Machining and Machinability of Materials*, *19*(6), pp.554-569.
14. Balakumar, S., Selvam, M.D. and Nelson, A.J.R., 2018. Wear and Friction Characteristics of Aluminium Matrix Composites Reinforced With Flyash/Cu/Gr Particles. *International Journal of ChemTech Research*, *11*(01), pp.121-133.
15. Selvam, M.D. and Sivaram, N., 2017. The Effectiveness of Various Cutting Fluids on the Surface Roughness of AISI 1045 Steel During Turning Operation Using Minimum Quantity Lubrication System. *Journal on Future Engineering & Technology*, *13*(1).
16. Selvam, M.D. and Sivaram, N.M., 2017. Optimal Parameter Design by Taguchi Method for Mechanical Properties of Al6061 Hybrid Composite Reinforced With Fly Ash/Graphite/Copper. *International Journal of ChemTech Research*, *10*(13), pp.128-137.
17. Thangamani, S.P., Ramasamy, K. and Dennison, M.S., 2018. The effect of cutting fluid on surface roughness of LM6 aluminium alloy during turning operation. *International Research Journal of Engineering and Technology (IRJET)*, *5*(2), pp.1198-1200.
18. Ponnusamy, R., Dennison, M.S. and Ganesan, V., 2018. EFFECT OF MINERAL BASED CUTTING FLUID ON SURFACE ROUGHNESS OF EN24 STEEL DURING TURNING OPERATION. *International Research Journal of Engineering and Technology (IRJET)*, *5*(2), pp.1008-1011.
19. Selvam, M.D. and Sivaram, N.M., 2018. A comparative study on the surface finish achieved during turning operation of AISI 4340 steel in flooded, near-dry and dry conditions. *Australian Journal of Mechanical Engineering*, pp.1-10.
20. DENNISON, M.S. and MEJI, M.A., 2018. A Comparative Study on the Surface Finish Achieved During Face Milling of AISI 1045 Steel Components. *i-Manager's Journal on Mechanical Engineering*, *8*(2), p.18.
21. Ramasamy, K., Dennison, M.S. and Baburaj, E., 2018. Surface Finish Achieved in Producing Pneumatic Piston Rod: An Experimental Investigation. *i-Manager's Journal on Mechanical Engineering*, *8*(3), p.9.
22. Vidyarthy, R.S., Dwivedi, D.K. and Muthukumaran, V., 2018. Optimization of A-TIG process parameters using response surface methodology. *Materials and Manufacturing Processes*, *33*(7), pp.709-717.
23. Alam, M.K., Urbanic, R.J., Nazemi, N. and Edrisy, A., 2018. Predictive modeling and the effect of process parameters on the hardness and bead characteristics for laser-cladded stainless steel. *The International Journal of Advanced Manufacturing Technology*, *94*(1-4), pp.397-413.

Author Brief Biography

Miniappan.P.K has obtained his bachelor and master degree in Mechanical Engineering from Bharathiar University and Karpagam Academy of Higher Education. Currently he is working as a Assistant Professor in Automobile Engineering. His area of interest includes welding and parameter optimization.

Published By:
Blue Eyes Intelligence Engineering
& Sciences Publication